### Title
Dynamic magneto-viscoelastic model for magnetorheological nanocomposites with imperfect interface




### Journal
International Journal of Damage Mechanics, 28(8)

### ISSN
1056-7895



### Authors
Chen, Xiangrong
Li, Rui
Sun, LZ



### Publication Date
2019-08-01

### DOI
10.1177/1056789518823877

Article

INTERNATIONAL JOURNAL OF DAMAGE MECHANICS

International Journal of Damage Mechanics
2019, Vol. 28(8) 1248–1260

DOI: 10.1177/1056789518823877
journals.sagepub.com/home/ijd
SAGE

# Dynamic magneto-viscoelastic model for magnetorheological nanocomposites with imperfect interface

**Xiangrong Chen[1,2], Rui Li[2] and LZ Sun[2]**

## Abstract

A dynamic magneto-viscoelastic interface model is proposed to study the effective magneto-mechanical responses of magnetorheological nanocomposites filled with carbon nanotubes. It is incorporated with the fundamental micromechanics principles, microstructural magnetic and mechanical coupling, and computational homogenization procedures. The field-dependent effective dynamic stiffness and damping of randomly dispersed, chain-structured nanocomposites are investigated with the consideration of imperfect interfacial conditions among nanofillers, micro-particles and the matrix. Comparisons are performed between the model prediction and experimental data for a specific type of Fe particle-reinforced elastomer nanocomposites filled with multi-walled carbon nanotubes to demonstrate the capability of the proposed model framework.

## Keywords

Nanocomposites, micromechanics, magneto-viscoelasticity, imperfect interface, homogenization

## Introduction

Magnetorheological elastomers (MREs) are adaptive elastomeric composites reinforced with ferromagnetic micro-particles. The addition of magnetizable particles allows magnetic fields to rapidly and continuously control the effective mechanical performance of the composites. Such tunable magnetorheological (MR) composites promise more functionality than conventional composites and therefore can provide a bridge among modern control technologies, intelligent structures, and robotics (Carlson and Jolly, 2000; Kim et al., 2018; Li et al., 2014; Lopez-Lopez et al., 2016; Elhajjar et al., 2018).

[1]School of Civil Engineering, Xi'an University of Architecture and Technology, Xi'an, China
[2]Department of Civil and Environmental Engineering, University of California, Irvine, CA, USA

**Corresponding author:**
LZ Sun, University of California, 4139 EG, Irvine, CA 92697-2175, USA.
Email: lsun@uci.edu

Development of MRE composites involves mixing and curing processes with liquid-state elastomer and ferrous micro-particles under steady magnetic fields (Jolly et al., 1996a). The ferrous particles are induced by the magnetic field to form chain-like structures, which then are embedded in the solidified rubber matrix. When such MR composites are exposed to an applied magnetic field, their bulk mechanical properties can be tailored by the magnetic field due to inter-particle magnetic interactions.

Because of their attractive properties (e.g. magnetostriction, stiffness, damping, and energy absorption), studies of magneto-mechanical responses for MREs are of great interest to researchers and engineers in many science and engineering disciplines. Experimentally, Ginder et al. (2002) investigated the magnetic field-dependent shear modulus of MREs by inducing shear deformation through sandwich cylinders with magnetostrictive composite cores. Zhou (2004) introduced a free-vibration method to measure the shear modulus of magnetic composites and extracted the complex shear modulus via a spectrum estimation method. Micromechanics-based modeling and simulation work on MR or magnetostrictive composites includes that of Davis (1999), who employed the dipole model and the finite element method to seek the maximum relative change of the shear modulus. Nan and Weng (1999) developed an effective-medium method for the magneto-elastic static behavior of such composites based on Green's function technique. Borcea and Bruno (2001) studied the magnetoelastic properties of elastomer composites filled with randomly oriented ferrous particles (not chain-structure) while Yin and Sun (2005a, 2005b) developed a micromechanics-based magneto-elastic model for chain-structured ferromagnetic composites. Liu et al. (2006) applied the constrained theory to calculate the effective elastic properties of the composites in the dilute limit.

While efforts have been made for MREs, the inferior mechanical response of the matrix materials (e.g. silicone rubber, natural rubber, and polybutadiene) severely inhibits their wide applications. During the last decade, a new generation of MRE-based nanocomposites filled with carbon nanotubes (CNTs) have been developed (Li and Sun, 2011). CNTs are allotropes of carbon with a cylindrical nanostructure and they possess attractive physical characteristics, making CNTs outstanding candidates of nanofillers for reinforcing polymers. Li and Sun (2014) further experimentally investigated the dynamic mechanical behavior of MR nanocomposites reinforced with multi-walled carbon nanotubes (MWCNTs), demonstrating that the MR nanocomposites show superiority not only in initial dynamic stiffness and damping behavior but also in the MR effects, compared with conventional MREs. Similar conclusions have been reported in Aziz et al. (2017) and Yang et al. (2016).

The advantages of MR nanocomposites over conventional MREs clearly exhibit their promising future in various types of applications. However, the corresponding underlying mechanisms and quantitative modeling have not been explored. Particularly, due to the limitation from fabrication techniques and large mechanical mismatch among constituents, imperfect viscoelastic interfaces (Chen et al., 2017, 2018a, 2018b; Li and Sun, 2013; Poniznik et al., 2017; Pupurs and Varna, 2017) exist not only between the matrix and CNTs but also between the matrix and iron particles. It is important to take account of interfacial debonding and interaction (Damiani and Sun, 2017; Dong et al., 2018; Heidarhaei et al., 2018; Ju and Yanase, 2009, 2011; Lee and Pyo, 2008, 2009; Luo et al., 2018; Paulino et al., 2006; Yanase and Ju, 2012) between reinforcing particles and the matrix that can affect the magnetic interaction among particles potentially leading to higher MR effect. Therefore, this paper aims to focus on the modeling and simulation of both zero-field and MR effect in dynamic shear stiffness and damping of the recently developed MR nanocomposites, which is the first trial to model and simulate the magneto-mechanical responses of the newly developed MR nanocomposites. Specifically a micromechanics-based interface model involving a two-step homogenization method is proposed, which utilizes the general viscoelastic interface model framework together with the magneto-viscoelastic effect. The effective dynamic stiffness and damping properties

of randomly dispersed, chain-structured MR nanocomposites are investigated with the consideration of imperfect interfacial conditions among nanofillers, micro-particles and the matrix. Comparisons are performed between the model prediction and experimental data for a specific type of Fe particle-reinforced elastomer nanocomposites filled with MWCNTs to demonstrate the capability of the proposed model framework.

## Modeling methodology

### *Viscoelastic interface with interfacial displacement jump*

For heterogeneous composites under consideration, particles and fillers (inhomogeneities) are randomly dispersed in the matrix material. During the fabrication process and under the applied external loading, particles may be debonded, causing imperfect interfaces between particles and the matrix. Interfacial bonding condition between inhomogeneities and the matrix plays an important role in determining the overall mechanical properties of composites. Imperfect interfaces may arise for various reasons such as thin coating layers, interfacial debonding, surface chemical reactions, etc. Mathematically speaking, for a perfect interface the displacement and traction fields are both continuous across the boundary of two phases, while for an imperfect interface this is not the case. Let us consider a two-phase medium occupying an infinite domain $D$, with the inhomogeneity phase occupying an ellipsoidal or spherical sub-domain $\Omega$. Let $S$ denote the interface between the two phases and $n_i$ its unit outward normal vector. For imperfect viscoelastic interfacial condition, Gosz et al. (1991) and Hashin (1991) introduced and Li and Sun (2013) modified a viscoelastic model with the time-dependent second-rank tensor $\eta_{ij}$ (representing the compliance of viscoelastic interface) as

$$\eta_{ij}(t) = \alpha(t)\delta_{ij} - \alpha(t)n_i n_j \tag{1}$$

and consequently the interfacial displacement jump (dependent on stress field $\sigma_{ij}$) is time-dependent as well, which can be written in an integral form

$$\Delta u_i(t) = \int_{-\infty}^{t} \eta_{ij}(t-\tau)\frac{\partial \sigma_{jk}(\tau)}{\partial \tau}\mathrm{d}\tau \cdot \Delta n_k \tag{2}$$

Composite materials show time-dependent modulus in creep and relaxation tests, and frequency-dependent modulus and damping under dynamic loads, provided that one or more phases are viscoelastic, or viscoelastic interfaces exist. A method to apply the correspondence principle is through the Fourier transform in which the stress–strain relations of the viscoelastic phases are transformed into frequency domain. Since viscoelastic materials do have frequency-dependent complex modulus, the frequency domain solution for modulus has direct physical meaning and does not need to be transformed back to time domain. Therefore, in case of finding harmonic viscoelastic solutions, e.g. effective complex modulus of the composite, we can simply replace the elastic modulus of each phase by the corresponding complex modulus in the elastic solutions. With the Fourier transform employed, the interfacial displacement jump–stress relation in equation (2) reads

$$\Delta u_i(\omega) = \int_{-\infty}^{\infty}\left[\int_{-\infty}^{t} \eta_{ij}(t-\tau)\frac{\partial \sigma_{jk}(\tau)}{\partial \tau}\mathrm{d}\tau\right]e^{-i\omega t}\mathrm{d}t \cdot \Delta n_k \tag{3}$$

with the complex interfacial compliance in the frequency domain as

$$\alpha^*(\omega) = \alpha'(\omega) - i\alpha''(\omega) \tag{4}$$

where the storage (real) and loss (imaginary) parts are respectively

$$\alpha'(\omega) = \alpha(\infty) - \omega \int_0^\infty [\alpha(\infty) - \alpha(t')] \sin(\omega t') \mathrm{d}t' \tag{5}$$

$$\alpha''(\omega) = \omega \int_0^\infty [\alpha(\infty) - \alpha(t')] \cos(\omega t') \mathrm{d}t' \tag{6}$$

As a result, in addition to replacing the elastic modulus of each phase by corresponding complex modulus, we may further use $\alpha^*(\omega)$ to obtain the complex modulus of composites with both viscoelastic phases and viscoelastic imperfect interfaces, if the solution for the elastic case is available.

## *Micromechanics and dynamic magneto-viscoelasticity of MR nanocomposites*

The developed smart MR nanocomposites are in essential three-phase viscoelastic composites (Figure 1), within which viscoelastic elastomer (e.g. silicone rubber) is the matrix phase and CNTs (e.g. MWNTs) and ferromagnetic particles (Fe particles) are the inhomogeneities showing elastic responses. While MWNTs are fiber-like and randomly oriented in the composites, spherical iron particles are aligned by the applied magnetic fields during the curing process to form chain-like structures, rendering the MR nanocomposites transversely isotropic. Due to the limitation in fabrication techniques, imperfect viscoelastic interfaces (Figure 1) exist not only between matrix elastomer and MWNTs (interface #1) but also between matrix elastomer and iron particles (interface #2).

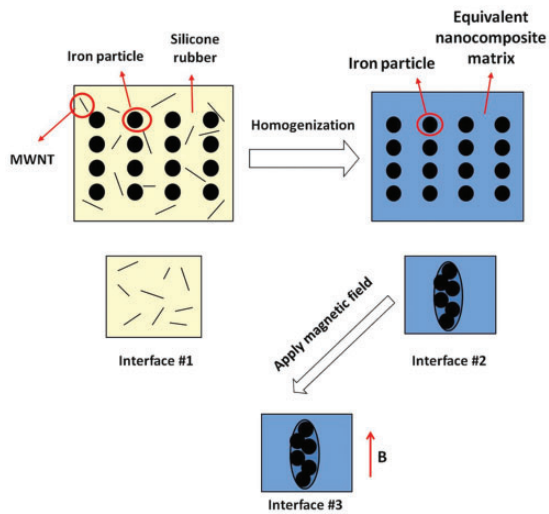


**Figure 1.** Illustration of the homogenization procedures in the proposed model and the interfacial condition at three different stages.

To model the zero-field dynamic viscoelastic properties of MR nanocomposites, a two-step homogenization method should be applied (Figure 1). In the first step, the matrix and MWNTs are treated as a two-phase nanocomposite with overall isotropic viscoelastic properties. The imperfect interfaces between MWNTs and the matrix (interface #1) are represented by the first set of appropriate interfacial parameters in this step. In the next step, the homogenized nanocomposite is regarded as a new matrix combining nanofillers and elastomer, and the three-phase MR nanocomposite is consequently modeled as a two-phase composite with chain-like iron particle structures embedded in the new matrix, showing the overall transverse isotropy. The second set of interfacial parameters has been used to characterize the imperfect interfaces (interface #2) between the new matrix and iron particle chains. Further, under magnetic fields, the iron particles are subjected to magnetic attractive forces along the chain direction from other particles within the chain, which affects the interfacial responses and therefore modifies the imperfect interface parameters (interface #3). The concept of this model is illustrated in Figure 1.

To accomplish the first step for two-phase nanocomposites filled with MWNTs, let us consider an ellipsoidal inhomogeneity $\Omega$ (phase 1 with stiffness tensor $C^1_{ijkl}$) embedded in medium $D$ (phase 0 with stiffness tensor $C^0_{ijkl}$). Furthermore, in case of an imperfect interface $S$, Qu (1993) has derived a modified Eshelby's tensor $S^M_{ijkl}$ which accounts for the imperfect interfacial compliance. Since the average perturbed strain over the inhomogeneity is sufficient for this study, the averaged $S^M_{ijkl}$ over $\Omega$ can be expressed as

$$\bar{S}^M_{ijkl} = S_{ijkl} + S_{ijmn}R_{mnpq}C^0_{pqst}(I_{stkl} - S_{stkl}) \tag{7}$$

where $S_{ijkl}$ is the original Eshelby tensor (Eshelby, 1957; Ju and Sun, 1999, 2001), and $I_{stkl}$ is the fourth-rank identity tensor. Further, the fourth-rank tensor $R_{mnpq}$ depends on the interfacial compliance and the geometry of the inhomogeneity, and can be written as

$$R_{mnpq} = \frac{1}{4\Omega}\int_s \left(\eta_{mp}n_q n_n + \eta_{mq}n_p n_n + \eta_{np}n_q n_m + \eta_{nq}n_p n_m\right)\mathrm{d}S \tag{8}$$

Now we apply the Mori–Tanaka method (Li and Sun, 2014; Mori and Tanaka, 1973) to solve the revised equivalent inclusion problem in which an elastic imperfect interface $S$ exists between the ellipsoidal inhomogeneity $\Omega$ and the infinite medium $D$. The effective overall stiffness tensor $\bar{C}_{ijkl}$ of two-phase nanocomposites can be derived as

$$\bar{C}_{ijkl} = C^0_{ijkl} + c_1 C^0_{ijmn}\left(A^{-1}_{mnpq} - R_{mnst}C^1_{stpq}\right)\left(c_1 R_{pqrs}C^1_{rskl} + I_{pqkl} + c_0\bar{S}^M_{pqrs}A^{-1}_{rskl}\right)^{-1} \tag{9}$$

where $c_0$ and $c_1$ are the volume fractions of the matrix and particles, respectively, and the fourth-rank elastic-phase-mismatch tensor $A_{ijkl} \equiv (C^1_{ijmn} - C^0_{ijmn})^{-1}C^0_{mnkl}$.

It is noted that the result in equation (9) gives the estimate for two-phase composites with aligned ellipsoidal inhomogeneities where $\bar{C}_{ijkl}$ is transversely isotropic. If all the inhomogeneities are randomly oriented in the composites, an orientational averaging process is needed which is defined as (Sun and Ju, 2004)

$$\langle\cdot\rangle \equiv \frac{1}{2\pi}\int_0^{2\pi}\int_0^{\pi/2}(\cdot)\sin\theta\mathrm{d}\theta\mathrm{d}\gamma \tag{10}$$

Upon the orientational averaging process, the effective overall elastic stiffness tensor $\bar{C}_{ijkl}$ of two-phase misoriented composites becomes isotropic and can be expressed as

$$\begin{aligned}\bar{C}_{ijkl} = C^0_{ijkl} + c_1 C^0_{ijmn}\left(A^{-1}_{mnpq} - \left\langle R_{mnst} C^1_{stpq}\right\rangle\right) \\ \times \left(c_1\left\langle R_{pqrs} C^1_{rskl}\right\rangle + I_{pqkl} + c_0\left\langle \bar{S}^M_{pqrs} A^{-1}_{rskl}\right\rangle\right)^{-1}\end{aligned} \tag{11}$$

It is further noted that, if the correspondence principle is applied and the elastic tensors in equation (11) are replaced by viscoelastic counterparts with complex components, the effective overall viscoelastic stiffness tensor $\bar{C}^*_{ijkl}$ is obtained. Given the complex shear modulus of matrix silicone rubber and the elastic constants, volume fraction, and aspect ratio of MWNT, in combination with interfacial parameters (interface #1), the complex stiffness tensor $\boldsymbol{C}^*_{\text{nano}}(\omega)$ of the two-phase nanocomposites reinforced with randomly oriented MWNTs is finally estimated through equations (7) to (11).

Subsequently, once the effective volume fraction of iron particles and the effective aspect-ratio of particle aggregations are assumed as well as a new set of interfacial parameters (interface #2), the complex stiffness tensor $\boldsymbol{C}^*_{3-\text{phase}}(\omega)$ of the three-phase MR nanocomposites with aligned particle aggregations are obtained from equation (9), with $\boldsymbol{C}^*_{\text{nano}}(\omega)$ treated as the property of the equivalent matrix. The dynamic shear stiffness $\bar{G}'_{3-\text{phase}}(\omega)$ and the loss factor $\overline{\tan\delta}_{3-\text{phase}}(\omega)$ can be consequently derived.

The magnetic field-induced change in dynamic stiffness and damping of MR nanocomposites is referred to as MR effect. The fundamental mechanism of the field-dependent viscoelastic responses of MR materials is the magnetic interaction among the ferromagnetic particles contained in these materials. The dipole–dipole magnetic interaction model developed by Jolly et al. (1996b) is applied here to simulate the MR effect on the dynamic shear stiffness $\Delta G$. As the magnetic field is applied, the interfacial condition (interface #3) at the interfaces between iron particle aggregations and the two-phase nanocomposite matrix is altered. The magnetic field-induced increases are depicted in storage shear modulus $\Delta\bar{G}'_{3-\text{phase}}(\omega)$, loss shear modulus $\Delta\bar{G}''_{3-\text{phase}}(\omega)$, and the loss factor $\Delta\overline{\tan\delta}_{3-\text{phase}}(\omega)$ as functions of applied frequency. It should be noted that the appropriate selection of interfacial parameters is the key factor to ensure the model success.

## Numerical simulations

Based on the modeling formulations and procedures described in the previous section, numerical simulations are performed on the basis of all equations from the previous section with no need of using finite element method and discretization. The results are compared with the experimental data (Li and Sun, 2014) for the dynamic mechanical behavior of MR nanocomposites filled with MWNTs. Figure 2 shows the comparisons between model predictions and experimental data for zero-field storage shear modulus and loss factor of MR nanocomposites with nominal iron particle volume fraction of 10% and 20%. The simulation data for the two-phase nanocomposites with the addition of 1 wt% MWNTs is also present for reference, which is the result of first step of homogenization described in the model. In consideration of consistency, the same parameters are used in the model from Li and Sun (2014): MWNTs are 20 nm in radius, 40 in aspect-ratio, and with Young's modulus of 200 GPa and Poisson's ratio of 0.2, while the first set of interfacial parameters are $\alpha_0(\omega) = \alpha'\left|G^*_0\right|/(2a) = 0.7$ and $\alpha''/\alpha' = 0.3$. In the second step of homogenization, the two-phase nanocomposites are regarded the equivalent matrix, and the same effective volume fractions and

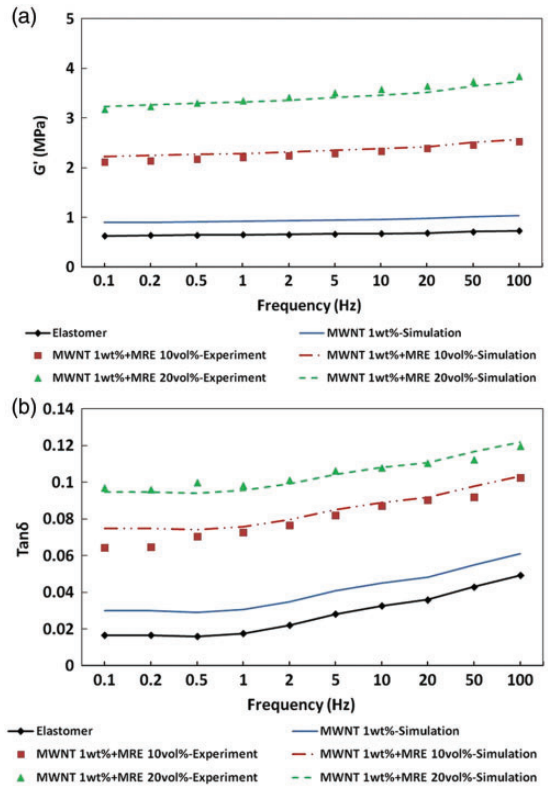


**Figure 2.** Comparisons between model predictions and experimental data for zero-field (a) storage shear modulus and (b) loss factor of MR nanocomposites.

**Table 1.** Effective volume fractions and interfacial parameters used in the simulation of zero-field dynamic viscoelastic properties of MR nanocomposites.

| Nominal volume fraction | | Effective volume fraction | Interfacial storage compliance $\alpha_0 = \alpha' \left\lvert G_0^*(\omega) \right\rvert / (2a)$ | Interfacial loss factor $\alpha''/\alpha'$ |
|---|---|---|---|---|
| MRE | 10% | 29% | 0.015 | 0.5 |
| | 20% | 44% | 0.012 | 0.45 |
| MR nanocomposite | 10% | 46% | 0.018 | 0.52 |
| | 20% | 61% | 0.015 | 0.48 |

MR: magnetorheological; MRE: magnetorheological elastomers.

effective aspect ratio of particle aggregations are used here. The second set of interfacial parameters are listed in Table 1, where their counterparts used for MREs are also given for comparison. It should be noticed that although the equivalent matrix are different for MREs and MR nanocomposites, the dimensionless parameter $\alpha_0$ which indicates the overall interfacial compliance is

**Table 2.** Interfacial parameters used in simulating the MR effect of MR nanocomposites.

| Nominal volume fraction | | Interfacial storage compliance $\alpha_0 = \alpha' \left\| G_0^*(\omega) \right\| / (2a)$ | | Interfacial loss factor $\alpha'' / \alpha'$ | | | |
|---|---|---|---|---|---|---|---|
| | | $B = 0$ T | $B = 0.2$ T | $B = 0$ T | $B = 0.2$ T | $k$ | $h$ |
| MRE | 10% | 0.015 | 0.02 | 0.5 | 0.6 | 4.5 | 1.06 |
| | 20% | 0.012 | 0.015 | 0.45 | 0.55 | 4.5 | 1.05 |
| MR nanocomposite | 10% | 0.018 | 0.02 | 0.52 | 0.66 | 4.5 | 1.05 |
| | 20% | 0.015 | 0.018 | 0.48 | 0.64 | 12 | 1.0 |

MR: magnetorheological; MRE: magnetorheological elastomers.

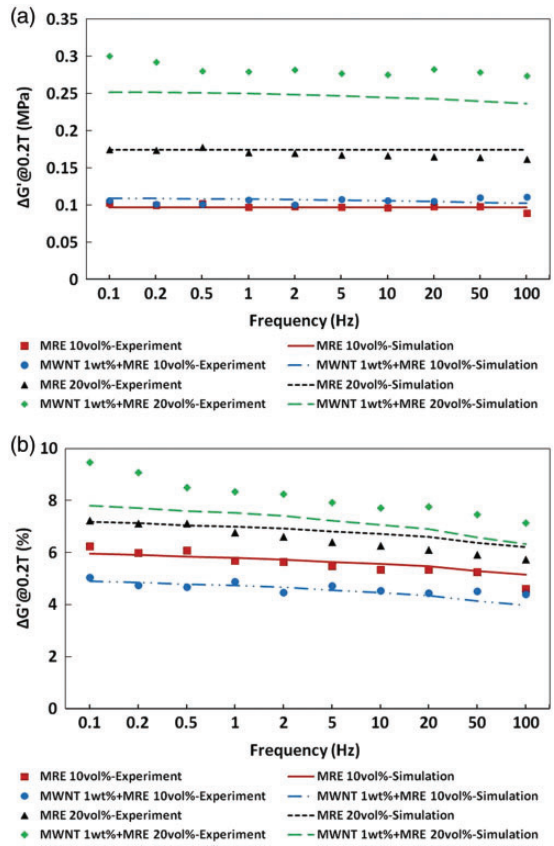


**Figure 3.** Comparisons between model predictions and experimental data for (a) absolute and (b) relative MR effect on storage shear modulus of MR nanocomposites.

constantly related with the complex modulus of silicone rubber, so that the values of $\alpha_0$ are directly comparable between the two cases. It is acknowledged that it is difficult to directly measure the interfacial parameters in experiments at two length scales. The interfacial data we use in Tables 1 and 2 are phenomenologically determined from the overall mechanical experiments of CNT

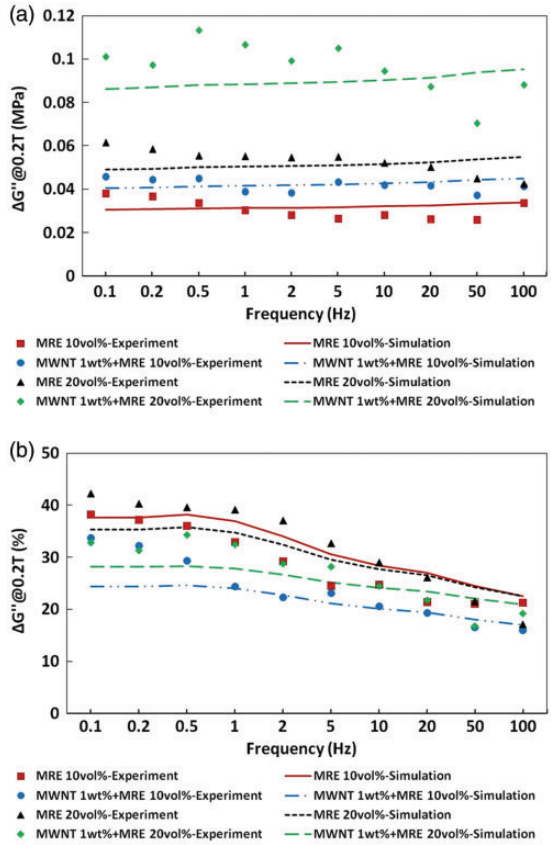


**Figure 4.** Comparisons between model predictions and experimental data for (a) absolute and (b) relative MR effect on loss shear modulus of MR nanocomposites.

nanocomposites and MR nanocomposites at a particular frequency. It can also be observed that, once the original matrix is modified by adding MWNTs, the interfacial condition between the matrix and iron particle aggregations is notably changed, in that it is overall more compliant and viscous for MR nanocomposites. The good agreement between simulation results and experimental data confirms the utility of this model in predicting the zero-field dynamic properties of MR nanocomposites.

Figures 3, 4, and 5 further demonstrate the comparisons between model predictions and experimental data for both absolute and relative MR effect on dynamic viscoelastic behavior of MR nanocomposites. The interfacial parameters for both MR nanocomposites and reference chain-structured MREs before and after the magnetic fields are applied are given in Table 2. Similar trends are found here for MR nanocomposites and MREs, in that both the interfacial storage compliance and loss factor are increased when external magnetic fields are applied. This observation further supports the explanation that the applied magnetic field disturb the stress field at the interfaces between particle aggregates and the matrix, which leads to weaker overall bonding yet higher viscosity at interfaces. However, although the parameters $k$ and $h$ in the dipole–dipole interaction model (Jolly et al. 1996b) have been adjusted to the maximum extent, the MR effect on the storage shear modulus of MR nanocomposites with 20% nominal particle volume fraction is still somehow

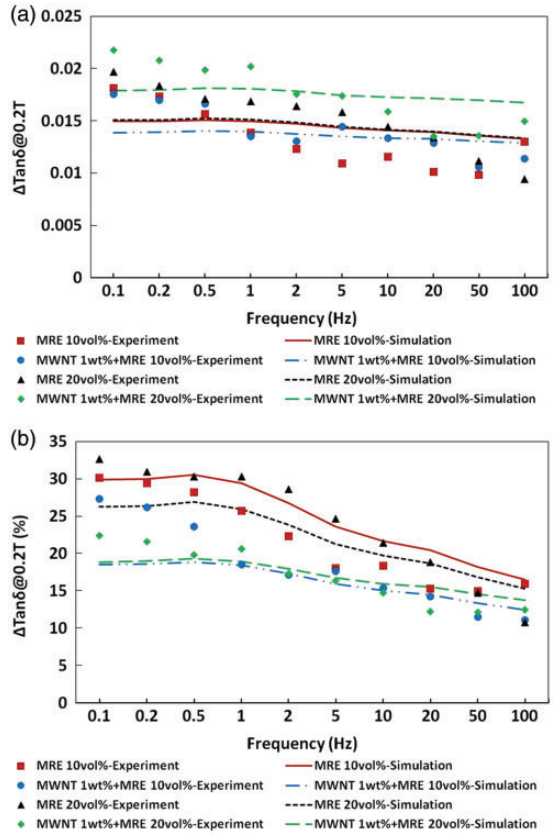


**Figure 5.** Comparisons between model predictions and experimental data for (a) absolute and (b) relative MR effect on loss factor of MR nanocomposites.

underestimated (approximately 10–18% difference for the entire frequency range from 0.1 to 100 Hz). The underlying mechanisms may be attributed to the magnetic interaction among the iron particles and MWNTs. Overall speaking, the simulation results have matched the overall trend of experimental data.

## Conclusions

In this paper, a micromechanics-based dynamic magneto-viscoelastic interface model is developed to investigate the effective magneto-mechanical responses of MR nanocomposites filled with CNTs. Both the zero-field dynamic viscoelastic behavior and the corresponding MR effect have been taken into account. A two-step homogenization approach is incorporated to address the two distinct reinforcing phases in the MR nanocomposites. The field-dependent effective dynamic stiffness and damping of randomly dispersed, chain-structured nanocomposites are investigated with the consideration of imperfect interfacial conditions among nanofillers, micro-particles and the matrix. Comparisons are conducted between the model prediction and experimental data for a specific type of Fe-particle-reinforced elastomer nanocomposites filled with MWCNTs to prove the validity of the proposed modeling framework. Specifically, the model predicts that the MR nanocomposites

have shown not only large jumps in zero-field dynamic stiffness and damping, but also higher magnetic field-induced improvement in these dynamic mechanical properties. The model is among the first efforts to construct the viscoelastic constitutive relation of three-phase nanocomposites incorporating the magneto-mechanical coupling. Simulations are performed to investigate the effects on the dynamic behavior of nanocomposites due to a couple of factors including interfacial storage compliance, interfacial damping, CNT aspect ratio, and CNT concentration. It is shown that the material interfaces play a significant role at both the microstructural length scales and macroscopic magneto-mechanical responses of the MR nanocomposites.

In the future research on MR nanocomposites, micromechanics-based modeling and simulation for the nonlinear viscoelasticity is a promising option to better understanding the viscoelastic behavior of smart nanocomposites under finite deformation. In terms of experimental efforts, testing configurations should be developed with capacity of generating wider range of magnetic field strength as well as temperature control, while improving fabrication techniques is a continuing objective.

## Declaration of conflicting interests

The author(s) declared no potential conflicts of interest with respect to the research, authorship, and/or publication of this article.

## Funding

The author(s) disclosed receipt of the following financial support for the research, authorship, and/or publication of this article: This work was partially sponsored by the National Science Foundation (NSF) under Grant CMMI-1229405. Further, X Chen's study at UC Irvine was partially supported by the China Scholarship Council (CSC).

## ORCID iD

LZ Sun http://orcid.org/0000-0001-9043-6526

## References

Aziz SAA, Mazlan SA, Ismail NIN, et al. (2017) An enhancement of mechanical and rheological properties of magnetorheological elastomer with multiwall carbon nanotubes. *Journal of Intelligent Material Systems and Structures* 28: 3127–3138.

Borcea L and Bruno O (2001) On the magneto-elastic properties of elastomer-ferromagnet composites. *Journal of the Mechanics and Physics of Solids* 49: 2877–2919.

Carlson JD and Jolly MR (2000) MR fluid, foam and elastomer devices. *Mechatronics* 10: 555–569.

Chen Q, Jiang Z, Zhu H, et al. (2017) Micromechanical framework for saturated concrete repaired by the electrochemical deposition method with interfacial transition zone effects. *International Journal of Damage Mechanics* 26: 210–228.

Chen Q, Jiang Z, Zhu H, et al. (2018b) A multiphase micromechanical model for unsaturated concrete repaired by electrochemical deposition method with the bonding effects. *International Journal of Damage Mechanics* 27: 1307–1324.

Chen Q, Zhu H, Ju JW, et al. (2018a) Stochastic micromechanical predictions for the effective properties of concrete considering the interfacial transition zone effects. *International Journal of Damage Mechanics* 27: 1252–1271.

Damiani R and Sun LZ (2017) Microstructural characterization and effective viscoelastic behavior of magnetorheological elastomers with varying acetone contents. *International Journal of Damage Mechanics* 26: 104–118.

Davis LC (1999) Model of magnetorheological elastomers. *Journal of Applied Physics* 85: 3348–3351.

Dong Y, Su C, Qiao P, et al. (2018) Microstructural damage evolution and its effect on fracture behavior of concrete subjected to freeze–thaw cycles. *International Journal of Damage Mechanics* 27: 1272–1288.

Elhajjar R, Law CT and Pegoretti A (2018) Magnetostrictive polymer composites: Recent advances in materials, structures and properties. *Progress in Materials Science* 97: 204–229.

Eshelby JD (1957) The determination of the elastic field of an ellipsoidal inclusion, and related problems. *Proceedings of the Royal Society of London Series A – Mathematical and Physical Sciences* 241: 376–396.

Ginder JM, Clark SM, Schlotter WF, et al. (2002) Magnetostrictive phenomena in magnetorheological elastomers. *International Journal of Modern Physics B* 16: 2412–2418.

Gosz M, Moran B and Achenbach JD (1991) Effect of a viscoelastic interface on the transverse behavior of fiber-reinforced composites. *International Journal of Solids and Structures* 27: 1757–1771.

Hashin Z (1991) Thermoelastic properties of particulate composites with imperfect interface. *Journal of the Mechanics and Physics of Solids* 39: 745–762.

Heidarhaei M, Shariati M and Eipakchi HR (2018) Effect of interfacial debonding on stress transfer in graphene reinforced polymer nanocomposites. *International Journal of Damage Mechanics* 27: 1105–1127.

Jolly MR, Carlson JD, Munoz BC, et al. (1996a) The magnetoviscoelastic response of elastomer composites consisting of ferrous particles embedded in a polymer matrix. *Journal of Intelligent Materials Systems and Structures* 7: 613–622.

Jolly MR, Carlson JD and Munoz BC (1996b) A model of the behavior of magnetorheological materials. *Smart Materials and Structures* 5: 607–614.

Ju JW and Sun LZ (1999) A novel formulation for the exterior-point Eshelby's tensor of an ellipsoidal inclusion. Journal of Applied Mechanics, *Transactions of ASME* 66: 570–574.

Ju JW and Sun LZ (2001) Effective elastoplastic behavior of metal matrix composites containing randomly located aligned spheroidal inhomogeneities, Part I: Micromechanics-based formulation. *International Journal of Solids and Structures* 38: 183–201.

Ju JW and Yanase K (2009) Micromechanical elastoplastic damage mechanics for elliptical fiber-reinforced composites with progressive partial fiber debonding. *International Journal of Damage Mechanics* 18: 639–668.

Ju JW and Yanase K (2011) Size-dependent probabilistic micromechanical damage mechanics for particle-reinforced metal matrix composites. *International Journal of Damage Mechanics* 20: 1021–1048.

Kim Y, Yuk H, Zhao R, et al. (2018) Printing ferromagnetic domains for untethered fast-transforming soft materials. *Nature* 558: 274–279.

Lee HK and Pyo SH (2008) Multi-level modeling of effective elastic behavior and progressive weakened interface in particulate composite. *Composites Science and Technology* 68: 387–397.

Lee HK and Pyo SH (2009) 3D-Damage model for fiber-reinforced brittle composites with microcracks and imperfect interfaces. *Journal of Engineering Mechanics* 135: 1108–1118.

Li R and Sun LZ (2011) Dynamic mechanical behavior of magnetorheological nanocomposites filled with carbon nanotubes. *Applied Physics Letters* 99: 131912-1–3.

Li R and Sun LZ (2013) A micromechanics-based viscoelastic model for nanocomposites with imperfect interface. *International Journal of Damage Mechanics* 22: 967–981.

Li R and Sun LZ (2014) Dynamic viscoelastic behavior of multi-walled-carbon-nanotube-reinforced magnetorheological nanocomposites. *ASCE Journal of Nanomechanics and Micromechanics* 4: A4013014–1-7.

Li Y, Li J, Li W, et al. (2014) A state-of-the-art review on magnetorheological elastomer devices. *Smart Materials and Structures* 23: 123001–1-24.

Liu LP, James RD and Leo PH (2006) Magnetostrictive composites in dilute limit. *Journal of the Mechanics and Physics of Solids* 54: 951–974.

Lopez-Lopez MT, Duran JDG, Iskakova LY, et al. (2016) Mechanics of magnetopolymer composites: A review. *Journal of Nanofluids* 5: 479–495.

Luo Q, Liu D, Qiao P, et al. (2018) Microstructural damage characterization of concrete under freeze-thaw action. *International Journal of Damage Mechanics* 27: 1551–1568.

Mori T and Tanaka K (1973) Average stress in matrix and average elastic energy of materials with misfitting inclusions. *Acta Metallurgica* 21: 571–574.

Nan CW and Weng GJ (1999) Influence of microstructural features on the effective magnetostriction of composite materials. *Physical Review B* 60: 6723–6730.

Paulino GH, Yin HM and Sun LZ (2006) Micromechanics-based interfacial debonding model for damage of functionally graded materials with particle interactions. *International Journal of Damage Mechanics* 15: 267–288.

Poniznik Z, Nowak Z and Basista M (2017) Numerical modeling of deformation and fracture of reinforcing fibers in ceramic–metal composites. *International Journal of Damage Mechanics* 26: 711–734.

Pupurs A and Varna J (2017) Steady-state energy release rate for fiber/matrix interface debond growth in unidirectional composites. *International Journal of Damage Mechanics* 26: 560–587.

Qu JM (1993) Eshelby tensor for an elastic inclusion with slightly weakened interface. *Journal of Applied Mechanics-Transactions of the ASME* 60: 1048–1050.

Sun LZ and Ju JW (2004) Elastoplastic modeling of metal matrix composites containing randomly located and oriented spheroidal particles. *ASME Journal of Applied Mechanics* 71: 774–785.

Yanase K and Ju JW (2012) Effective elastic moduli of spherical particle reinforced composites containing imperfect interfaces. *International Journal of Damage Mechanics* 21: 97–127.

Yang P, Yu M and Fu J (2016) Ni-coated multi-walled carbon nanotubes enhanced the magnetorheological performance of magnetorheological gel. *Journal of Nanoparticle Research* 18: 61.

Yin HM and Sun LZ (2005a) Magnetoelasticity of chain-structured ferromagnetic composites. *Applied Physics Letters* 86: 261901-1–3.

Yin HM and Sun LZ (2005b) Elastic modeling of periodic composites with particle interactions. *Philosophical Magazine Letters* 85: 163–173.

Zhou GY (2004) Complex shear modulus of a magnetorheological elastomer. *Smart Materials and Structures* 13: 1203–1210.